Modelling the Cone Penetration Test in Sand Using Cavity Expansion and Arbitrary Lagrangian Eulerian Finite Element Methods

A. Tolooiyan

School of Architecture, Landscape and Civil Engineering, University College Dublin

K. Gavin

School of Architecture, Landscape and Civil Engineering, University College Dublin

Abstract:

The paper set out two techniques to model the Cone Penetration Test (CPT) end resistance, q_c in a dense sand deposit using commercial finite element programmes. In the first approach, Plaxis was used to perform spherical cavity expansion analyses at multiple depths. Two soil models, namely; the Mohr-Coulomb (MC) and Hardening Soil (HS) models were utilized. When calibrated using simple laboratory element tests, the HS model was found to provide good estimates of q_c. However, at shallow depths, where the over-consolidation ratio of the sand was highest, the relatively large horizontal stresses prevented the full development of the failure zone resulting in under-estimation of the q_c value. The second approach involved direct simulation of cone penetration using a large-strain analysis implemented in Abaqus/Explicit. The Arbitrary Lagrangian Eulerian (ALE) technique was used to prevent excessive mesh deformation. Although the Druker-Prager soil model used was not as sophisticated as the HS model, excellent agreement was achieved between the predicted and measured q_c profiles.

Keywords: Cone penetration test, Finite element analysis, Cavity expansion, Arbitrary Lagrangian Eulerian, Over-consolidated sand

1 Introduction

The Cone Penetration Test (CPT) is a widely used geotechnical site investigation test. In the test a standard 60° cone is pushed into a soil deposit at a rate of 20 mm/sec and the cone end resistance q_c, sleeve side friction f_s and porewater pressure are monitored continuously (See Lunne et al 1997). Because side friction measurements tend to be variable many correlations have been developed between q_c and soil properties or through correlations with design values for various geotechnical structures (e.g. the end bearing resistance of piles). In order to maximise the usefulness of the CPT and refine correlations, a number of analytical approaches have been developed to model cone penetration. Janbu and Sennesset (1974), Houlsby and Wroth (1982) and others have considered the problem as analogous to the limit equilibrium problem of the bearing capacity of a circular footing. Yu and Mitchell (1998) noted that since the effects of soil compressibility and stress changes along the pile shaft caused by pile installation were ignored, the method had limited application. Bishop et al. (1945) introduced limit pressure solutions for cavity expansion and this has been applied widely to model the penetration resistance of piles and penetrometers (Vesic 1972), Yu et al. (1996) and Salgado et al. (1997). Randolph et al. (1994) considered the vertical equilibrium of stresses at the tip of an advancing pile (See Figure 1). By expanding a cavity of finite radius, a limiting pressure (p_{limit}) is achieved. This is related to the unit end resistance q_b or cone tip stress q_c:

[1] $$q_c = p_{limit} (1+ \tan\theta . \tan\phi)$$

Where θ is the cone angle and ϕ is the friction angle of the soil.

Recent developments in computer technology have led to the application of Finite Element Methods (FEM) to penetrometer modelling. A range of constitutive models can now be applied to complex soil geometries in small and more recently large-strain analyses. Yu et al. (2000) developed a technique to simulate steady state cone penetration. In their method, the penetrometer was placed in a pre-bored hole and only a few steps of penetration were modelled. This approach neglects transient deformation of the soil body around the cone. Susila and Hryciw (2003), Huang et al. (2004) and Liyanapathirina (2009) considered the use of large-strain FEM analysis to examine cone penetration in normally consolidated soils. Contact elements were used at the soil-pile interface to allow penetration to large depths to be achieved, and to investigate the effect of soil properties such as ϕ on the q_c value.

A limitation of most of the approaches outlined above is that calibration between the predicted q_c resistance and field measurements is rarely performed. A notable exception was the work described by Xu (2007) and Xu and Lehane (2008) who used cavity expansion analyses performed using the finite element package Plaxis to consider the effect of soil layering on the mobilised pile base resistance (q_b) value. Xu (2007) employed the linear-elastic perfectly plastic Mohr Coulomb (MC) and the non-linear Hardening Soil (HS) model and found that both soil models gave results which where closely comparable to results obtained with a closed-form solution proposed by Yu and Houlsby (1991). The MC model assumes a constant elastic stiffness (E) to represent soil displacements for stresses up to the yield stress. Salgado et al. (1997) noted that since the cavity expansion limit pressure is significantly affected by soil non-linearity, the MC model is of limited practical significance. The HS model is an advanced, hyperbolic soil model formulated in the framework of hardening plasticity. The non-linear stiffness is defined by using three input stiffness parameters, E_{50} which represents the stiffness measured in a triaxial

compression test when the shear stress (τ) is 50% of the maximum shear stress (τ_{max}), the triaxial unloading stiffness (E_{ur}) and E_{oed}, which is derived from an oedometer test.

This paper compares q_c profiles predicted using FEM analyses to CPT q_c profiles measured at University College Dublin (UCD) dense sand test bed site located at Blessington, County Wicklow. The FEM profiles were derived by performing spherical cavity expansion analyses using the MC and HS constitutive models available in Plaxis version 8 (2002) and large-strain FEM analyses performed using Abaqus/Explicit version 6.9 (2009). The latter analyses used the Arbitrary Lagrangian Eulerian (ALE) method to allow large deformation analyses to be performed without numerical and mesh instability occurring. A description of the calibration of the soil models using laboratory element tests performed is presented. In the final part of the paper, the predicted q_c profiles are compared with those measured at the UCD test site.

2 Soil Conditions

The UCD dense sand test bed site is located in Blessington, County Wicklow approximately 25 km south-west of Dublin. The deposit is in an over-consolidated state due to glacial action, ground water level changes, and recent sand extraction. The maximum pre-consolidation stress estimated from oedometer tests is ≈ 800 kPa. Extensive CPT testing has been performed at the site in association with model pile and footing tests described by Gavin and O'Kelly (2007), Gavin and Lehane (2007) and Gavin et al. (2009). CPT profiles for the site are illustrated in Figure 2a whilst shear wave velocity v_s measured using the Multi-Channel Analysis of Surface Waves (MASW), see Donohue et al. (2003) is shown in Figure 2b. The small strain shear modulus G_0 can be estimated from the v_s profile if the soil bulk unit weight (γ_b) is known:

[2] $G_0 = \gamma_b \cdot v_s^2$

The water table was approximately 13 m below the ground level (bgl) at which the CPT profiles were measured. The natural water content of samples taken at 0.5 m intervals between ground level and 4 m bgl were relatively constant at 10 – 12%. The unit weight of the material calculated from sand replacement tests was 20 kN/m^3 , and the degree of saturation was 71%. In order to provide input parameters for FEM soil models, triaxial compression tests and oedometer tests on representative soil samples were required. A smooth, thin-walled stainless steel 100 mm diameter sampling tube with a bevelled end was pushed into the sand deposit using the 20 tonne CPT rig as reaction. Whilst full recovery was obtained (with the sample length being equal to the tube penetration), the sample proved to be extremely difficult to remove from the tube using conventional procedures resulting in sample disturbance occurring. As an alternative, a reconstituted sample was formed using the procedure described by Tolooiyan (2010). In this method a PVC cylinder (with a diameter of 50 mm and length 100 mm), which was lubricated on the inside surface, was filled with sand at the natural moisture content. The sample which was compacted into layers using a vibrating hammer was then placed in an modified oedometer cell (See Figure 3a). A vertical pressure of 800 kPa was then applied for a period of days. The sample was then extruded into a triaxial membrane (see Figure 3b). A series of triaxial and oedometer tests were performed at a range of cell pressures on samples reconstituted using this technique in order to determine the strength and stiffness characteristics of the sand. The triaxial tests revealed that the constant volume friction angle of this well-graded, angular sand was 37°, and the dilation angle which varied with the confining pressure, was 5.4° at the reference pressure of 100 kPa.

The elastic stiffness (E) was derived from the G_0 profiles using Eqn. 3, where the possions ratio ν, was assumed to be equal to 0.2:

[3] $$G_0 = \frac{E_0}{2(1+\nu)}$$

The coefficient of earth pressure at rest was estimated from using Eqn. 4 (from Terzaghi et al. 1996):

[4] $$K_o = (1-\sin\phi_{cv}) \times (OCR)^{\sin\phi_{cv}}$$

Where, ϕ_{cv} is the constant volume friction angle and OCR is over-consolidation ratio.

3 Cavity Expansion Analyses using Plaxis

3.1 Calibration of FEM model

A calibration procedure of the FE models was undertaken in which the laboratory oedometer and triaxial compression test results were modelled using Plaxis. The oedometer test was modelled in an axisymmetric analysis of unit dimensions (1 m x 1 m), See Figure 4a. The soil was assumed to be weightless and therefore the dimensions considered did not influence the result. The left-hand boundary was the axis of symmetry and normal displacements were restrained at the bottom right-hand and left hand boundaries, whilst tangential displacements were free. In the calculation phase the sample was loaded vertically and the model parameters E_{oed}^{ref} and the power m, which described the stress dependent stiffness according to Eqn. 5 were varied until a reasonable match to the measured laboratory test results was obtained, see Figure 4b.

[5] $$E_{oed}^{ref} = \left(\frac{\sigma}{p_{ref}}\right)^{m}$$

The triaxial test was modelled using the same sample size as the oedometer sample. The boundary conditions were changed wherein normal displacements were restrained at the left and bottom boundaries whilst tangential displacements were free. The calculation was performed in two stages. In the first stage, an all-round cell pressure of 100 kPa was applied. Having set the displacements to zero, the second stage involved loading the sample to failure by increasing the vertical stress whilst maintaining a constant horizontal stress. Since the parameters E_{oed}^{ref} and m were known from the oedometer calibration and the oedometer unload-reload stiffness E_{ur}^{ref} was measured in the oedometer test, the E_{50}^{ref} value was varied until a reasonable match with the experimental data was obtained (See Figure 5). The MC and HS parameters used for modelling Blessington sand are summarised in Table 1.

3.2 FEM model

Spherical cavity expansion analyses were performed to estimate p_{limit} and hence estimate q_c using Eqn. 1. Axisymetric analyses were performed using the mesh shown in Figure 6. The left-hand boundary was the axis of symmetry, the vertical and horizontal boundaries were fixed at the base, and horizontal displacements were restrained at the right-hand boundary. The mesh was 10 m wide and 21 m deep. Rather than perform cavity expansion analyses at a number of depths within the soil mesh, significant numerical efficiencies were achieved by placing a 1 m dummy layer at the top of the 20 m deep weightless soil deposit. By varying the unit weight of the

dummy layer, uniform stress conditions in the soil sample were achieved. The effect of increasing confining pressure (or depth) was achieved using uniform mesh comprising of 15 noded triangular elements with 12 gauss points per element. In order to minimise computational resources, Tolooiyan (2010) reported a sensitivity analysis which concluded that a minimum of 472 elements were required in order to negate boundary effects.

The analyses were completed using a procedure similar to that described by Xu (2007) and Xu and Lehane (2008) which included four steps:

Step 1 *Material Set-Up and Initial Stresses* - Material parameters were assigned to the appropriate model from Table 1. The initial vertical stress conditions were determined by varying unit weight of the dummy layer material and the horizontal stress was calculated using Eqn. 4.

Step 2 *Cavity Expansion* – The spherical cavity was expanded using small-step increases in volumetric strain. Automatic mesh updating was used to minimise calculation errors.

Step 3 *Extraction of Results* – The data were integrated with radial effective stresses being determined based on average data from nine nodes and principal stresses from ten stress points inside the cavity.

Step 4 *Post-Processing* – The data tables were exported to excel and the radial strain and average principal stress was calculated. The graphs of principal stress versus radial strain were prepared and the limit pressure was determined, (see Figure 7).Using this procedure, q_c values were

determined for depth ranges between 0.3 m and 10 m bgl using the HS model and between 2 m and 7 m bgl using the MC model. The values predicted using the HS and MC models are compared in Figure 8, where it is clear that the results from the MC model are very sensitive to the stiffness value E used in the analysis. In contrast the HS model, which was implemented using the soil properties derived from the lab test calibration procedure, provided a reasonably good estimate of the measured CPT q_c profile. At a given depth, the analysis time using the HS model were significantly longer than runs using the MC model. One average run-time using the HS model took one hour. Given that 10 depth intervals were typically used, the time required to produce a q_c profiles was approximately 12 hours.

4 Large Strain Analysis using Abaqus

4.1 FEM Model

The Abaqus finite element package utilising the Arbitrary Lagrangian Eulerian method was used to analyse CPT q_c values to 10 m bgl at the Blessington test site. Due to the large number of elements required to model the installation of a 36 mm penetrometer to such a relatively large depth, and the consequent significant computational time required, the actual soil element considered in the analysis was 1500 mm wide and 3000 mm deep. Multiple analyses for different depth intervals were performed where the vertical overburden stress over the soil cluster were changed to model the stress state which would occur during penetration in each depth interval. An axisymmetric model which included 35946 elements and 36244 nodes was considered (See Figure 9). The main part of soil cluster is modelled using CAX4R element which is 4-node, reduced-integration, axisymmetric element, while the bottom and right boundary is modelled

using CINAX4 which is 4-node, axisymmetric, infinite element (See Figure 9). The 18 mm radius cone with a cone angle of 60° and the CPT body was modelled using two independent analytical rigid surfaces. This allowed the stresses generated by the cone tip to be separated from friction developed along the cone sleeve.

Whilst some workers (Susila and Hryciw 2003 and Liyanapathirana 2009) modelled the start of the cone penetration from the base of a pre-formed borehole, in the analyses presented here, penetration starts at the ground surface in an effort to fully consider the effect of near surface horizontal stresses. The insitu vertical stress and k_o value was prescribed using Abaqus/CAE Keywords Editor and soil material assumed weightless. Whilst left boundary is an axis of symmetry and it is allowed to only have positive radial displacement and bottom and right boundaries assumed infinite, only the given vertical overburden stress will control the depth independent uniform stress conditions in the soil cluster.

4.2 ALE Re-meshing Technique

Because of the large deformations caused during penetrometer installation, a re-meshing technique is required in order to avoid excessive mesh distortion. The ALE technique was employed in the analyses described herein. ALE technically combines the features of pure Lagrangian analysis and pure Eulerian analysis by allowing the mesh to move independently of the material and makes it possible to maintain a high-quality of mesh even when very large deformation happens. Whilst a range of options are available in Abaqus/Explicit to implement ALE, the Volume Smoothing (VS) method was adopted. The VS approach relocates a node position by computing a volume weighted average of the centre of elements surrounding the

node (Abaqus 2009). This technique is illustrated in Figure 10, where the new position of node M is determined from the position of the element C1 to C4. VS will tend to push the node M away from C1 and towards C3, thus reducing element distortion. Only elements which are close to high strain area adjacent to the penetrometer require ALE (see Figure 9a). Significant computational run-time savings can be achieved if normal meshes are used in zones where relatively low strains are experienced.

4.3. FEM Calibration for ALE Analysis

The non-associative linear Drucker-Prager (DP) model was employed in Abaqus/Explicit to model the soil elements. The DP yield surface which is described in the *p–t* plane is shown in Fig. 11. The failure and flow potential criterion are expressed in Eqns. 7 and 8, respectively, where β is friction angle, d is cohesion and ζ is dilation angle in the *p-t* plane.

[7] $$F = t - p\tan\beta - d = 0$$

[8] $$G = t - p\tan\zeta$$

For triaxial conditions the mean stress, p and deviator stress, t are:

[9] $$t = \sigma_1 - \sigma_3$$

[10] $$p = \frac{1}{3}(\sigma_1 + 2\sigma_3)$$

The results of three triaxial tests, performed at cell pressures of 20kPa, 50kPa and 100kPa respectively, which suggests that d is zero and β is ≈ 56° are shown in Figure 12. Alternatively it is possible to convert the MC friction angle to the DP friction angle using Eqn. 11, which yields an estimated β value of 56.4° when ϕ=37°.

[11] $$\tan\beta = \frac{6\sin\phi}{3-\sin\phi}$$

The DP model uses a constant stiffness E. In order to choose a representative value, the stress level dependent stiffness response of the triaxial tests was considered. The deviator stress-strain response of a sample tested at a mean stress of 50 kPa is shown in Figure 13a. Line A represents failure at constant volume. A secant stiffness measured from the start of the stress-strain curve to point b which is the intercept of the failure surface, suggests that a single secant stiffness value provides a relatively good fit to the measured response. The variation of this secant stiffness with stress level is shown in Figure 13b, and this was used to provide an input secant stiffness for the FE modeling.

4.4. Modeling Cone-Soil and Sleeve-Soil interface

The steel CPT cone and sleeve were modeled by analytical rigid surface which penetrated into the deformable soil. By default the Abaqus/Explicit assigned the pure master-slave kinematic contact algorithm to the cone-soil and sleeve-soil interface. In this mode the cone and sleeve are the master surface, and whilst the master penetrates the slave elements, the slave elements cannot penetrate the master, making this an ideal tool for penetrometer modeling. Due to the very large

displacements involved, the master surface tracks nodes in the slave surface using a search algorithm known as the *contact tracking algorithm,* See Abaqus (2009). The interface friction angle (δ) at the soil-cone and soil-sleeve interface was set as 50% of friction angle and the coefficient of friction (μ) is used in Abaqus where:

[12] $$\mu = \tan \delta$$

4.5. Estimated q_c Profile using ALE Analysis

The cone and sleeve were pushed into the sand at a displacement rate of 20 mm/s. The vertical reaction force of rigid cone reference point was logged at 0.1 second intervals and following penetration the force and displacement values were exported to an excel file. The vertical reaction force developed by the cone was divided by cone cross section area then used to produce a q_c profile. The performance of the ALE technique is maintaining the integrity of the mesh is illustrated in Figure 14a which shows the deformed mesh following 400 mm penetration of the cone. The CPT q_c profiles predicted for a penetration depth of 6 m bgl at the Blessington test site are shown in Figure 14b. It is clear that the q_c value achieved a steady state value at a penetration of approximately 200 mm (approximately eleven penetrometer radii). The steady state q_c value of $\approx$ 17.5 MPa was used to produce the q_c versus depth profile. The time required to penetrate the cone through 250 mm was five minutes (using a PC with a 2.2 GHz dual channel processor). The CPT q_c profile derived using this procedure is seen to be closely comparable to the measured profile in Figure 14c.

5. Comparison between CEM and ALE q_c Analysis in Blessington Sand

The q_c profiles predicted using both the CEM and ALE methods are compared to the measured CPT q_c profiles in Figure 15. The ALE method is seen to produce a reasonable lower-bound estimate of q_c for depths up to 10 m bgl. The CEM method tended to under-predict the q_c value at shallow depths (< 2 m), and became more accurate as the penetration depth increased. To investigate the cause of the under-prediction at shallow depths, the effect of depth (or stress level) on the development of plastic strains is considered in Figure 16. As the depth increased from 0.3 m bgl (K_o = 7.54) to 6 m bgl (K_0 = 1.25), it is clear from Figure 16 that a full spherical plastic failure zone did not develop around the cavity for depths < 2 m (or K_0 values > 2). This resulted in an underestimate of p_{limit} and therefore q_c in this region. Below this depth both the CEM and ALE methods were broadly comparable.

Although the number of elements in the Abaqus model was 76 times greater than in the Plaxis model, the analysis time required was only 8% of that required by Plaxis. This is partly due to the fact that Abaqus utilized dual channel processing which increased its computational efficiency. However, the HS model in Plaxis is also more sophisticated than the DP model in Abaqus, which although incorporated the effect of stress level on stiffness, it did not include a strain level dependence. The excellent prediction achieved using the DP model is at least in part due to the relatively weak pre-yield stress dependence of E on strain level evident in Figure 13a for the heavily over consolidated sand at Blessington. The method is unlikely to provide such good predictions for materials which exhibit more highly non-linear stiffness degradation (See

Atkinson 2000 and Gavin et al. 2009), where the use of more sophisticated models should be considered.

6. Summery and Conclusion

This paper compared the q_c profiles measured in over consolidated sand with profiles predicted using commercially available FE packages. Plaxis was used to perform spherical cavity expansion analyses which yielded the limit pressure which was then converted to q_c. Two stiffness models were considered, the Mohr-Coulomb (MC) and Hardening Soil (HS) models. Although it was possible to predict a reasonable q_c profile with the MC model when a stiffness of 50% of the small strain stiffness was adopted, the choice of this assigned constant stiffness value was somewhat arbitrary and site specific. The HS model allows for a realistic non-linear soil stiffness to be specified and provided good estimates of q_c values at depths greater than 2 m bgl or when the K_0 value was lower than 2. For higher K_0 values, relatively high horizontal stresses prevented the development of a fully plastic spherical failure zone, and the cone resistance was underestimated.

A more direct approach to CPT modeling was performed using Abaqus/Explicit. The use of an auto adaptive remeshing technique (ALE) allowed the large-strain problem of cone penetration to be modeled without unacceptable mesh distortion. Excellent predictions of the CPT q_c resistance were obtained, albeit with a relatively simple Druker-Prager soil model, which is not as robust as the HS model available in Plaxis.

The relatively good agreement between predicted and measured q_c profiles achieved was due in part to careful calibration of all of the soil models using laboratory element tests performed on carefully prepared samples on Blessington sand. Significant computational efficiencies were obtained by creating finite element models which considered only small depths, where techniques such as the use of dummy layer in Plaxis and stress controlled boundary conditions in Abaqus allowed the effect of stress level or depth to be modelled.

Acknowledgements

We acknowledge the assistance of Paul Doherty and David Igoe of the School of Architecture, Landscape and Civil Engineering of University College Dublin in undertaking the fieldwork, and Dr. Eric Farrell of Trinity College Dublin who provided the CPT profiles. We also wish to thank Roadstone Ltd for the use of the quarry at Blessington, Co. Wicklow.

References:

Abaqus, Ver. 6.9. (2009). Dassault Systèmes Simulia Corp., Providence, RI, USA.

Atkinson, J.H. 2000. Non-linear soil stiffness in routine design. Géotechnique, 50: 487–508.

Bishop, R. F., Hill, R., and Mott, N. F. (1945). The theory of indentation and hardness tests. The Proceeding of the Physical Society. Vol. 57, Part 3, No. 321.

Donohue, S., Gavin, K., Long, M., and O'Connor, P. (2003). Determination of the shear stiffness of Dublin boulder clay using geophysical techniques. *In* Proceedings of the 13th European

Conference on Soil Mechanics and Geotechnical Engineering, Prague, Czech Republic, 25–28 August 2003. *Edited by* I. Vanicek, R. Barvinek, J. Bohac, D. Jirasko, and J. Salak. The Czech Geotechnical Society, Prague, Czech Republic. Vol. 3, pp. 515–520.

Gavin, K.G., and O'Kelly, B.C. (2007). Effect of friction fatigue on pile capacity in dense sand. Journal of Geotechnical and Geoenvironmental Engineering, 133 (1):63-71

Gavin, K.G., and Lehane, B.M. (2007). Base Load-Displacement Response of Piles in Sand. Canadian Geotechnical Journal, 44 (9):1053-1063.

Gavin, K., Adekunte, A., and O'Kelly, B. (2009). A field investigation of vertical footing response on sand. Proceedings of the Institution of Civil Engineers-Geotechnical Engineering, 162 (5):257-267.

Houlsby, G.T., Wroth, C.P. (1982). Determination of undrained strengths by cone penetration tests. Proceedings of the 2nd European Symposium on Penetration testing, vol. 2. p. 585–90.

Huang, W., Sheng, D., Sloan, S.W., and Yu, H.S. (2004). Finite element analysis of cone penetration in cohesionless soil. Computers and Geotechnics. 31, p. 517–528.

Janbu, N., and Senneset, K. (1974). Effective stress interpretation of in situ static penetration tests. Proceedings of the 1st European Symposium on Penetration Testing. vol. 2. p. 181–93.

Liyanapathirana, D. S. (2009). Arbitrary Lagrangian Eulerian based finite element analysis of cone penetration in soft clay. Computers and Geotechnics 36, p. 851–860

Lunne, T., Robertson, P.K., and Powell, J.J.M. (1997). Cone Penetration Testing in Geotechnical Practice, Blackie Academic and Professional, Chapman and Hall, London, p.312.

Plaxis, Ver. 8. (2002). Delft University of Technology & Plaxis b. v., The Netherlands.

Randolph, M. F., Dolwin, J., and Beck, R. (1994). Design of drivenpiles in sand. Geotechnique 44, No. 3, 427–448.

Salgado, R., Mitchell, J.K., and Jamiolkowski, M. (1997). Cavity expansion and penetration resistance in sand. ASCE J Geotech Geoenv Eng. 123(4), p. 344–54.

Susila, E. and Hryciw, R.D. (2003). Large Displacement FEM Modeling of the Cone Penetration Test (CPT) in Normally Consolidated Sand. International Journal for Numerical and Analytical Methods in Geomechancis, Vol. 27, No. 7, pp. 585-602.

Terzaghi, K., Peck, R. B. and Mesri, G., Soil Mechanics in Engineering Practice, 3rd Ed. Wiley-Interscience (1996) ISBN 0-471-08658-4, p. 105.

Tolooiyan, A. (2010). Pressure-Settlement models for cohesionless soils. PhD thesis in preparation, University College Dublin, Ireland.

Vesic, A. S. (1972). Expansion of cavities in infinite soil mass. ASCE Journal of the Soil Mechanics and Foundations Division, 98:265–90.

Xu, X. (2007). Investigation of the end bearing performance of displacement piles in sand. PhD thesis, The University of Western Australia.

Xu, X. & Lehane, B. M. (2008). Pile and penetrometer end bearing resistance in two-layered soil profiles. Geotechnique, 58, No. 3, p.187–197.

Yu, H. S., and Houlsby, G. T. (1991). Finite cavity expansion in dilatant soils: loading analysis. Geotechnique 41, No. 2, 173–183.

Yu, H. S., and Mitchell, J.K. (1998). Analysis of cone resistance: a review of methods. Journal of Geotech Geoenv Eng ASCE. 124(2), p.140–9.

Yu H.S., Schnaid, F., and Collins, I. F. (1996). Analysis of cone pressuremeter tests in sands. J Geotech Eng ASCE, 122(8), p. 623–32.

Yu, H. S, Herrmann L. R and Boulanger R. W. (2000). Analysis of steady cone penetration in clay. Journal of Geotech Geoenv Eng ASCE.;126(7), p. 594–605.

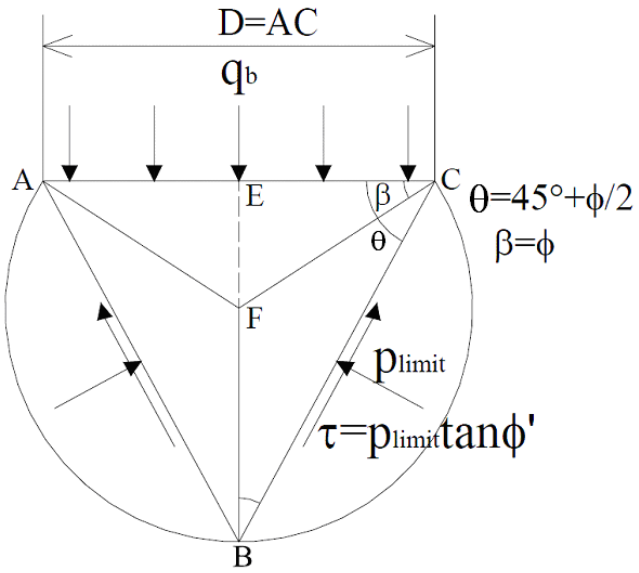

Fig. 1. Randolph et al. (1994) relationship between tip resistance q_b and cavity limit pressures P_{limit}

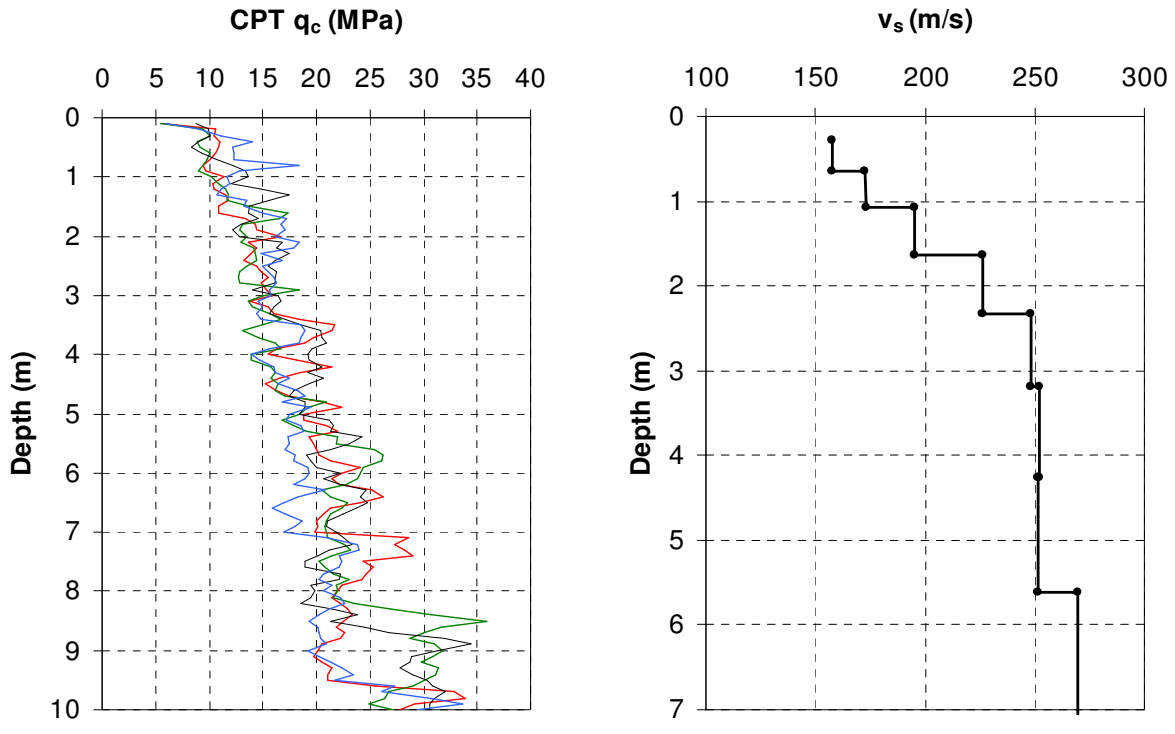

(a) (b)

Fig. 2. CPT q_c profile (a) and v_s profile using MASW (b) of Blessington sand

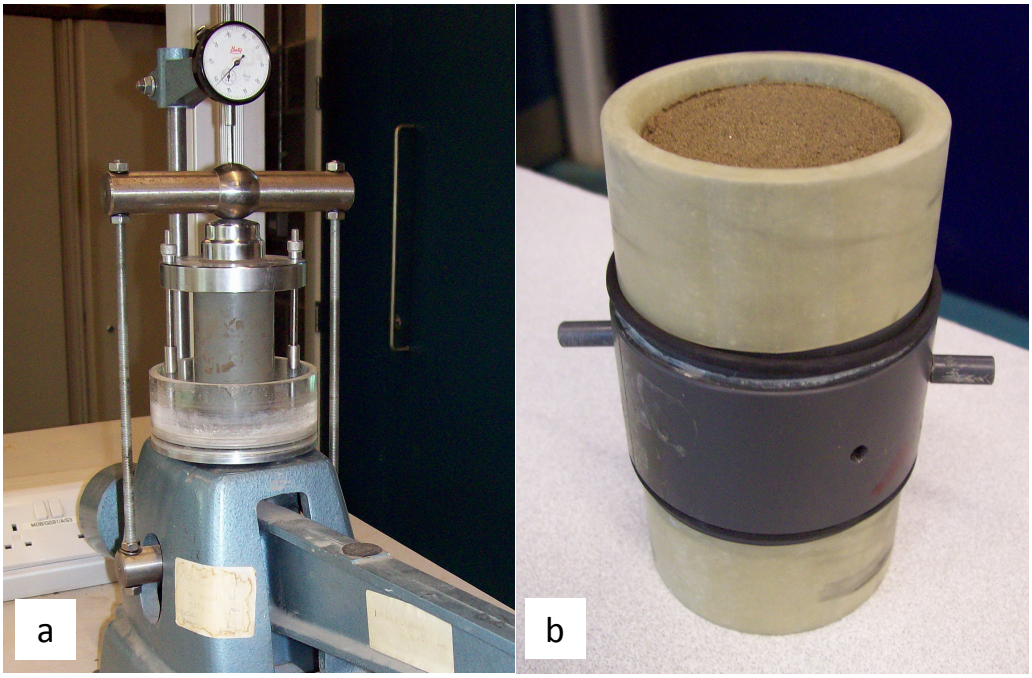

Fig. 3. Triaxial sample preparation (Tolooiyan, 2010)

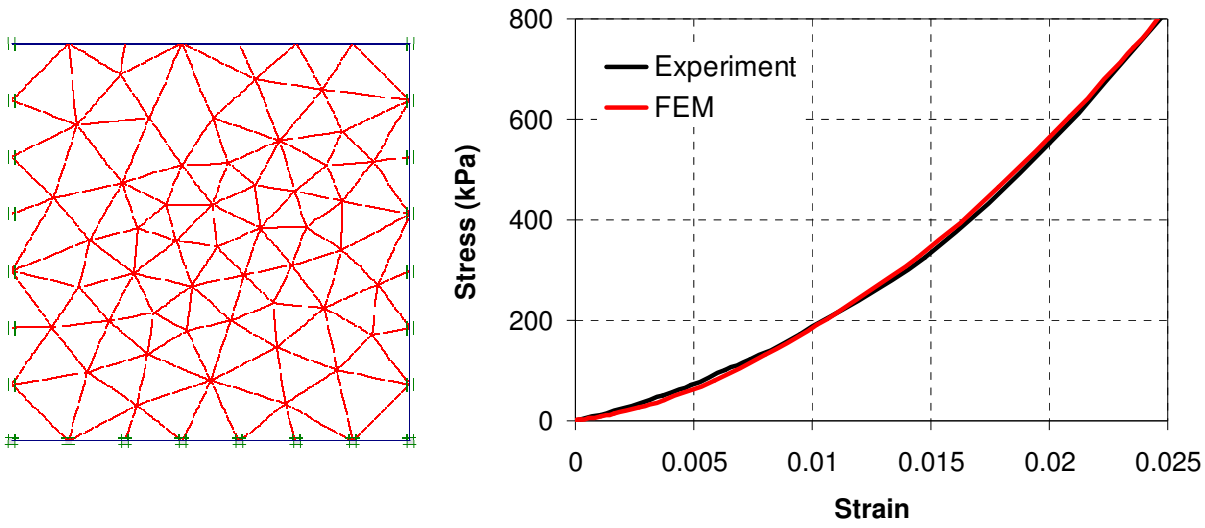

(a) (b)

Fig. 4. Oedometer test FEM geometry (a), Comparison of experimental and FEM oedometer test (b)

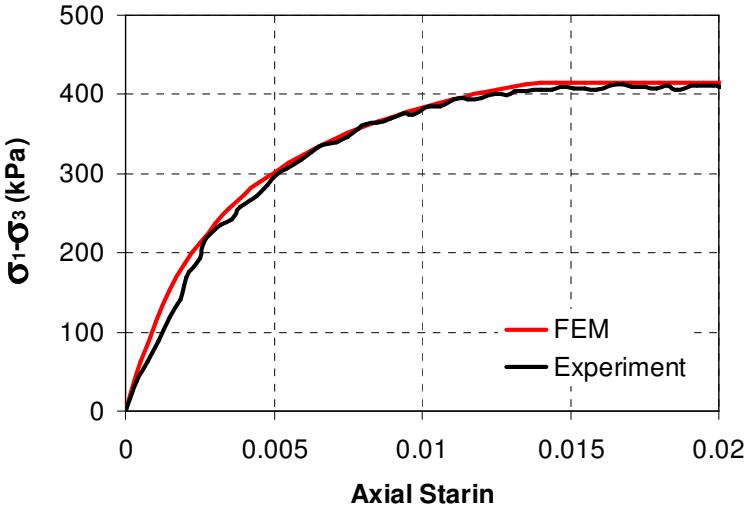

Fig. 5. Comparison of experimental and FEM triaxial test

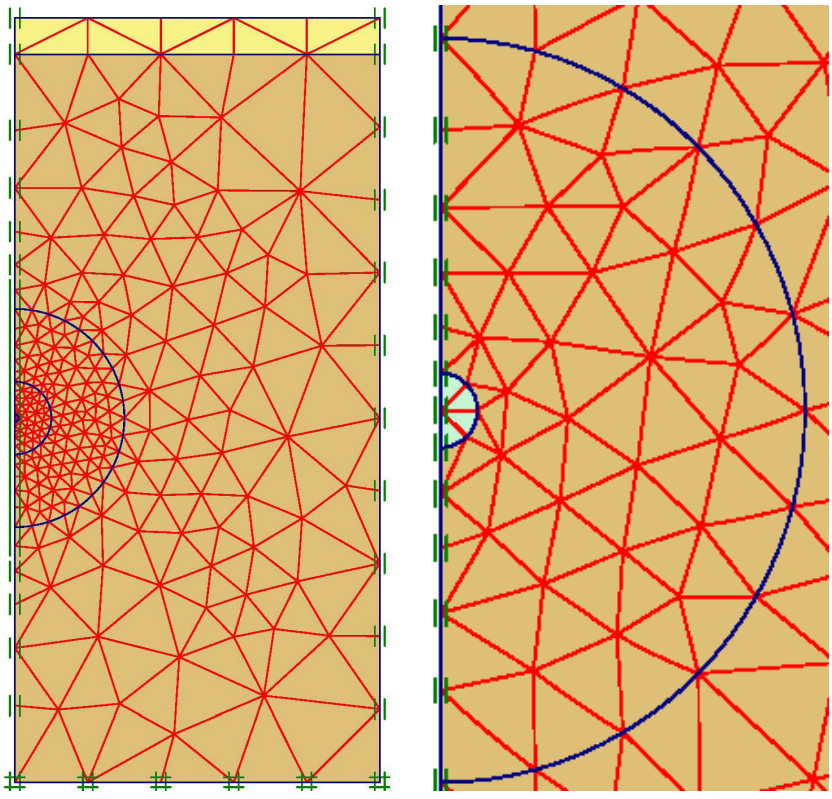

Fig. 6. Plaxis FEM geometry and cavity area

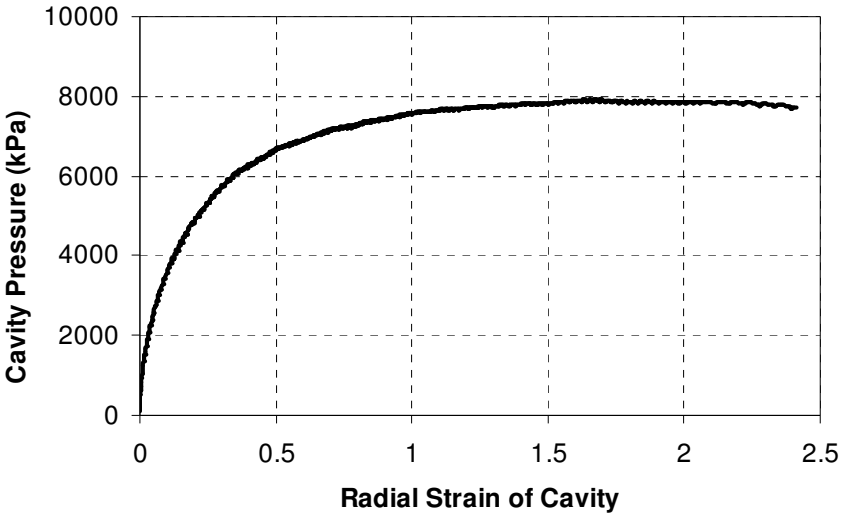

Fig. 7. Cavity expansion analysis in 2m depth of Blessington sand using MC model

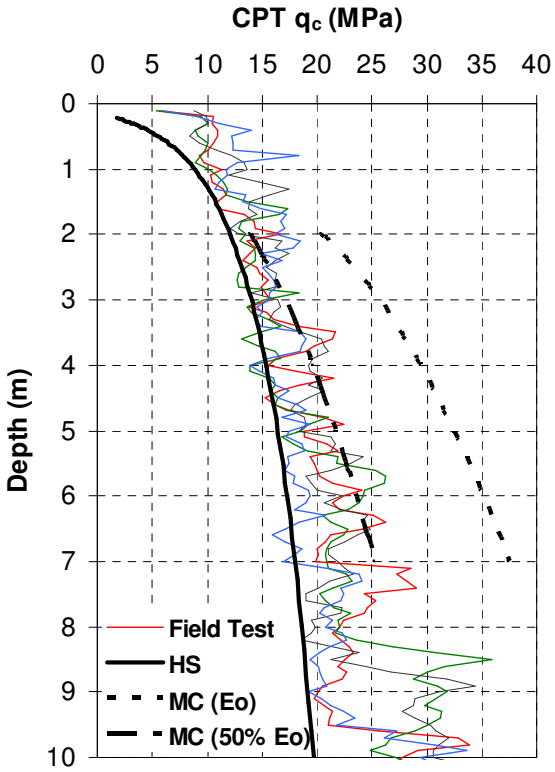

Fig. 8. CPT q_c profile estimated using cavity expansion analysis

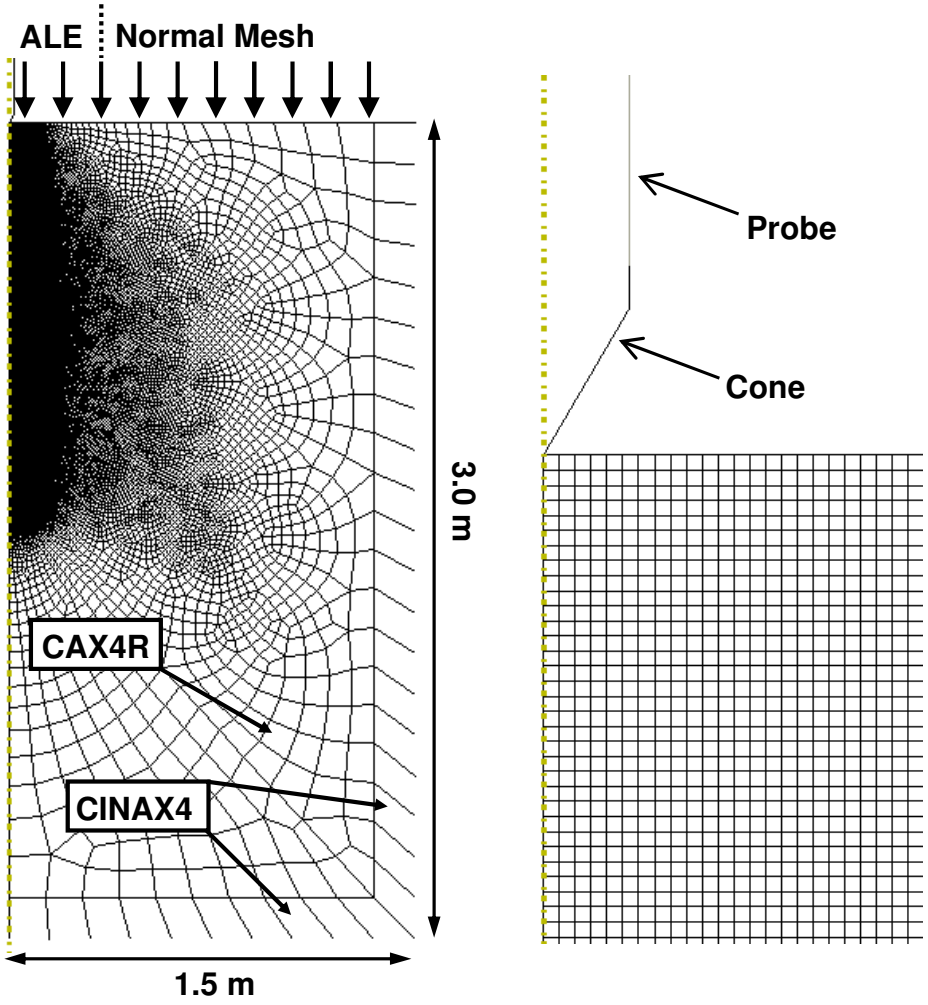

Fig. 9. Geometry of CPT finite element analysis in Abaqus

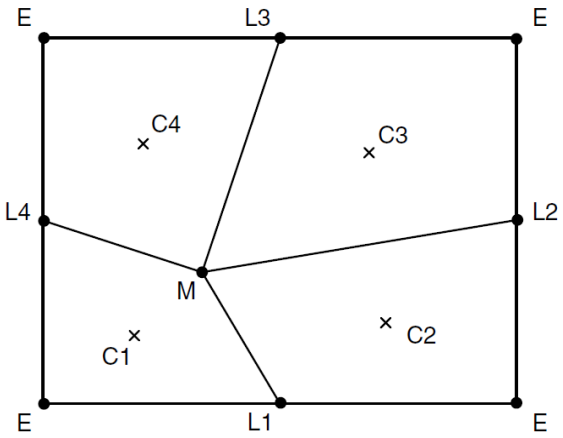

Fig. 10. Volume smoothing method in Abaqus/Explicit (Abaqus, 2009)

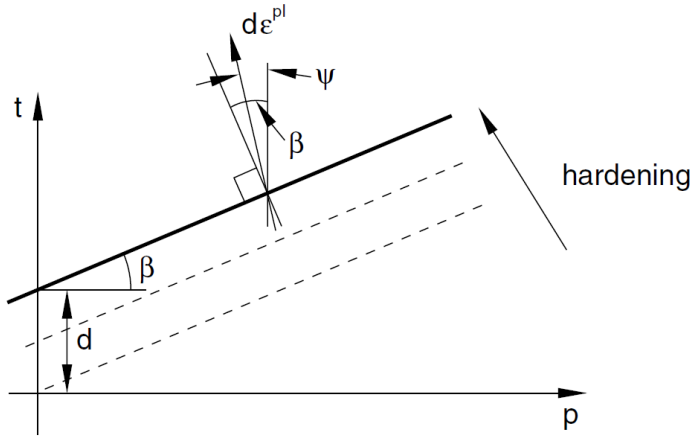

Fig. 11. Yield surface and flow direction in the p–t plane (Abaqus, 2009)

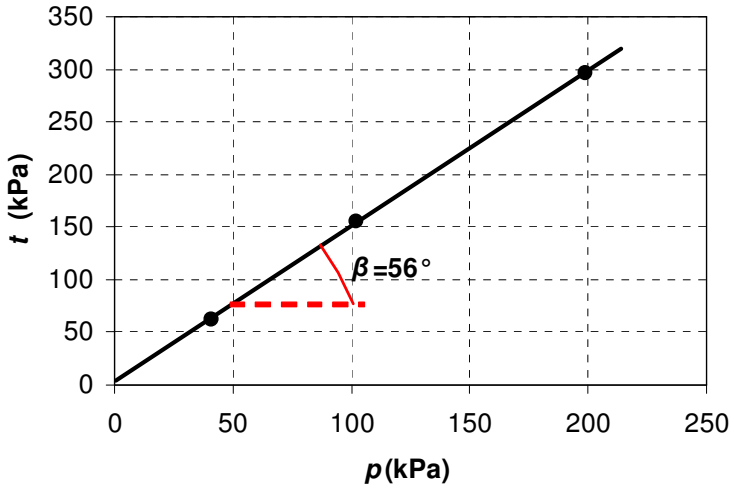

Fig. 12. Triaxial test results in *p*-*t* plane

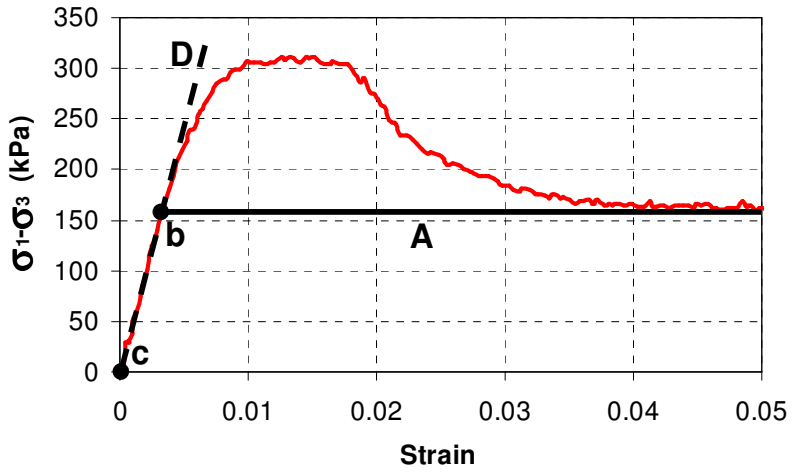

(a)

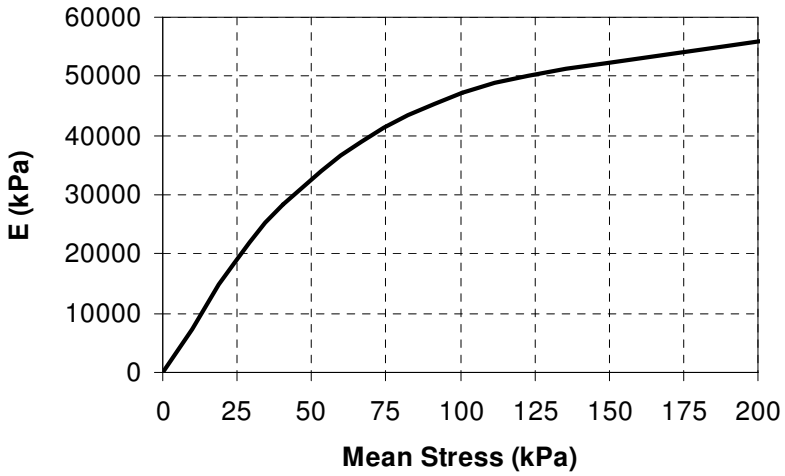

(b)

Fig. 13. Stiffness of Blessington sand in 50kPa triaxial test (a) and in at varying mean stress levels (b)

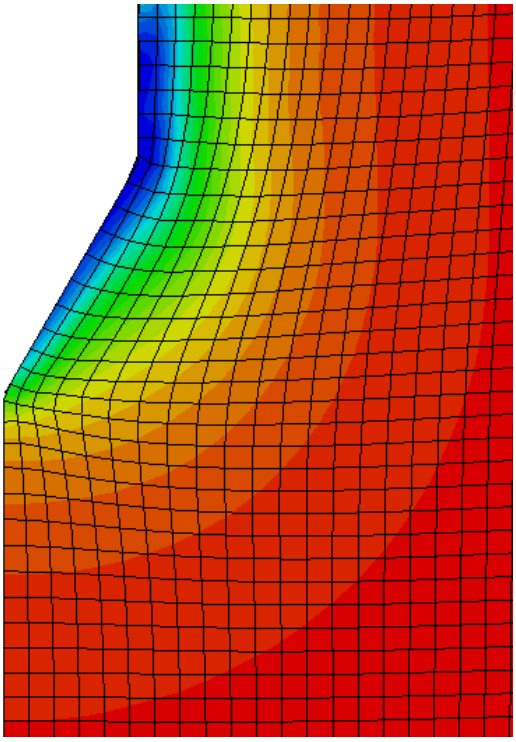

(a)

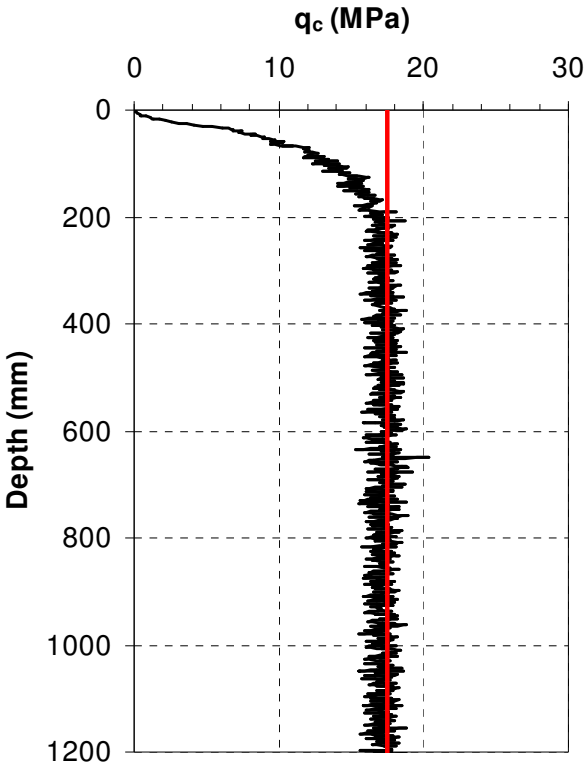
q_c (MPa)
0
10
20
30
0
200
400
600
800
1000
1200
Depth (mm)

(b)

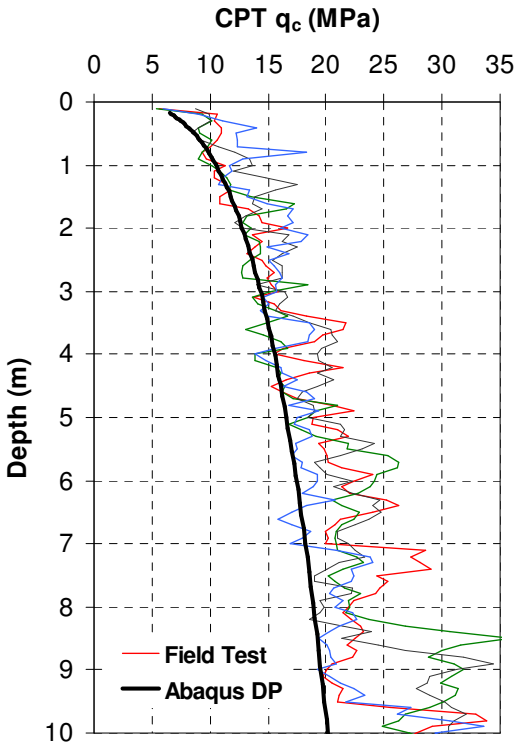
CPT q_c (MPa)
0
5
10
15
20
25
30
35
0
1
2
3
4
5
6
7
8
9
10
Depth (m)
Field Test
Abaqus DP

(c)

Fig. 14. FE mesh after installation(a), CPT q_c value at 6m depth of Blessington sand (b), CPT q_c profile developed by ALE analysis (c)

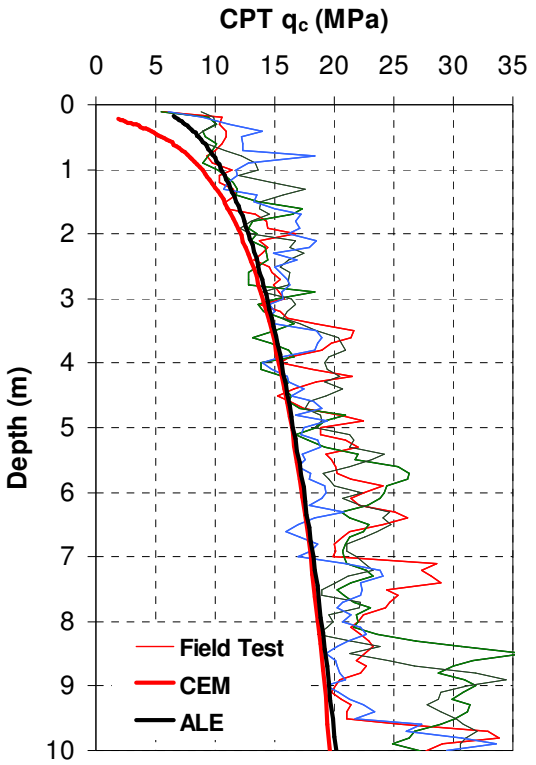

Fig. 15. Comparison between actual q_c profiles and profiles estimated by CEM and ALE

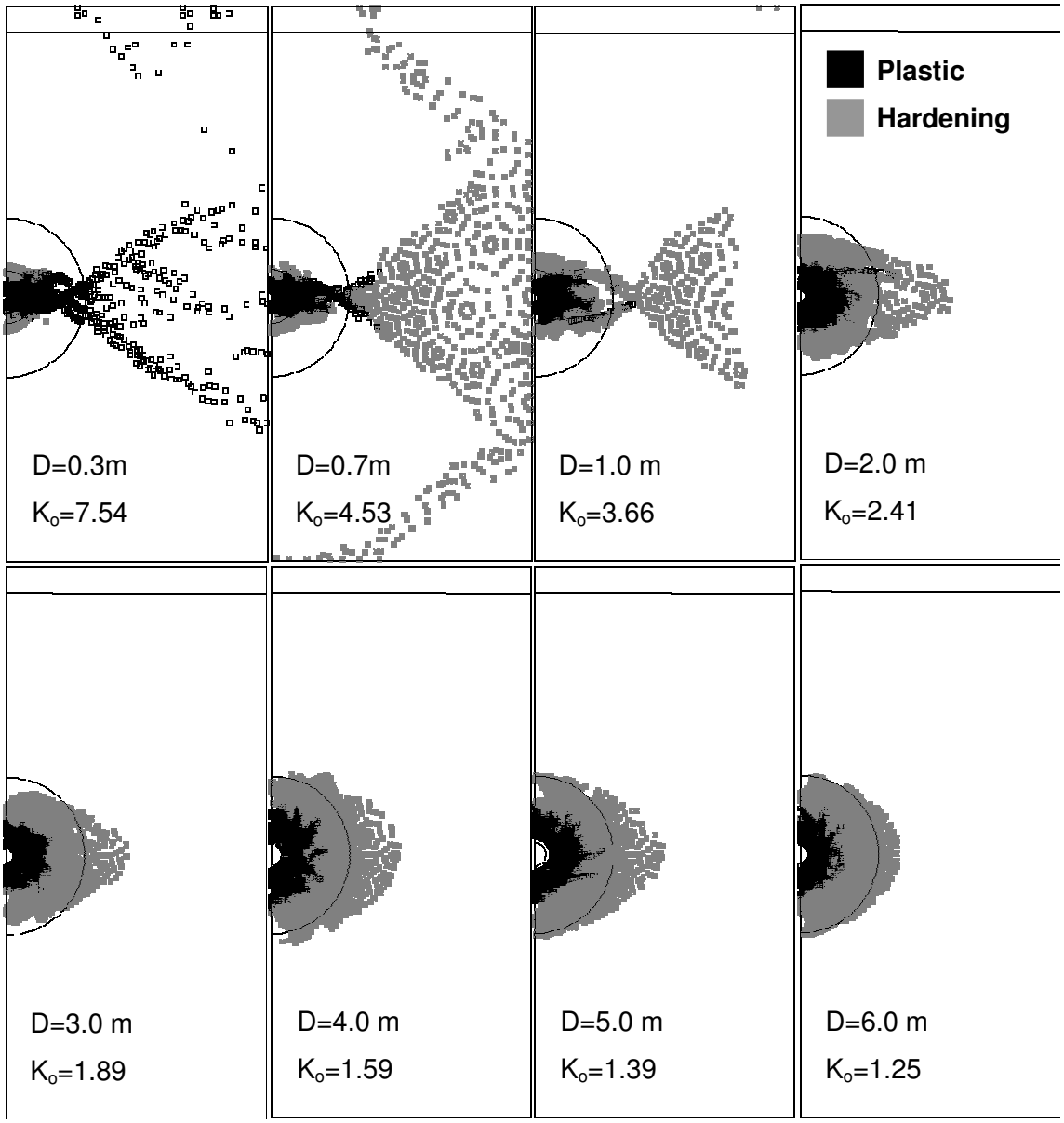

Fig. 16. Plastic region around the cavity at P_{limit} pressure at different depth of Blessington sand

Table 1. MC and HS parameters of Blessington sand

Parameter	MC	HS
Unit Weight γ(kN/m^3)	20	20
E_{50}^{ref} (P_{ref}=100kPa) (kPa)	-	44000
E_{ur}^{ref} (P_{ref}=100kPa) (kPa)	-	155000
E_{oed}^{ref} (P_{ref}=100kPa) (kPa)	-	25000
E	Variable by depth	-
Cohesion (kPa)	0.0	0.0
Ultimate Friction angle (°)	42.4	42.4
Ultimate Dilatancy angle* (°)	6.6	6.6
Poisson's ratio	0.2	0.2
Power m	-	0.4
R_f	-	0.8
Tensile Strength (kPa)	0.0	0.0
e_{init}	0.373	0.373
e_{min}	0.373	0.373
e_{max}	0.733	0.733
Dr (%)	100	100
P_{ref} (kPa)	-	100

* Ultimate dilatancy angle (ψ_m) has been estimated using $\sin\psi_m = \left(\frac{\sin\phi_m - \sin\phi_{cv}}{1 - \sin\phi_m \sin\phi_{cv}}\right)$

Table 2. Drucker-Prager parameters of Blessington sand

Parameter	Value
d (kPa)	0
β (°)	56.4
E (kPa)	Variable
k	1
v	0.2